Vol 17 No 10, October 2008
1674-1056/2008/17(10)/3827-09

Chinese Physics B

Formation and photoluminescence properties of boron nanocones*

Wang Xing-Jun(王兴军)[a], Tian Ji-Fa(田继发)[a], Bao Li-Hong(鲍丽宏)[a], Yang Tian-Zhong(杨天中)[a], Hui Chao(惠 超)[a], Liu Fei(刘 飞)[b], Shen Cheng-Min(申承民)[a], Xu Ning-Sheng(许宁生)[b], and Gao Hong-Jun(高鸿钧)[a]†

[a] *Beijing National Laboratory for Condensed Matter Physics, Institute of Physics, Chinese Academy of Sciences, Beijing* 100190, *China*

[b] *State Key Laboratory of Optoelectronic Materials and Technologies, School of Physics and Engineering, Sun Yat-sen University, Guangzhou* 510275, *China*

(Received 22 February 2008; revised manuscript received 11 April 2008)

This paper reports that a simple chemical vapour deposition method has been adopted to fabricate large scale, high density boron nanocones with thermal evaporation of B/B_2O_3 powders precursors in an Ar/H_2 gas mixture at the synthesis temperature of 1000–1200°C. The lengths of boron nanocones are several micrometres, and the diameters of nanocone tops are in a range of 50–100 nm. transmission electron microscopy and selected area electron diffraction indicate that the nanocones are single crystalline α-tetragonal boron. The vapour–liquid–solid mechanism is the main formation mechanism of boron nanocones. One broad photoluminescence emission peak at the central wavelength of about 650 nm is observed under the 532 nm light excitation. Boron nanocones with good photoluminescence properties are promising candidates for applications in optical emitting devices.

Keywords: boron nanocones, chemical vapour deposition, photoluminescence
PACC: 6140M, 8115H, 7855C

1. Introduction

One-dimensional nanomaterials of semiconductors are of great interest because of their potential fundamental and practical applications in many areas such as electronics, magnetics, optoelectronics, thermoelectrics, and photonics, etc.[1−3] Among one-dimensional nanomaterials of semiconductors, boron is an unique element with structure complexity due to the electron-deficient nature of boron.[4,5] Extensive research of bulk boron and boron based materials has been reported. Boron is the third lightest solid element in the Periodic Table, a low density of 2.340 g/cm^3, but with a high melting point of 2300°C, a high Young's modulus of 380–400 GPa, and as well as a high hardness close to diamond.[6−8] Recent experimental results show that boron may become metallic under a pressure of about 160 GPa at room temperature, and transform from a nonmetal to a superconductor at 6 K. The critical temperature of transition increases from 6 K to 11.5 K when we further increase the pressure up to 250 GPa.[9] Boron based compounds also exhibit many interesting physical and chemical properties. For example, the superconducting in MgB_2 above 39 K has been discovered by Larbalestier *et al.*[10] Lanthanum hexaboide (LaB_6) single crystals have been one of the most widely used thermionic electron sources in a large variety of devices requiring electron emission. In the past decade, the theoretical and experimental studies about one-dimensional boron and boron based compound nanomaterials have been also extensively developed. Some theoretical studies have suggested that the existence of layered, tubular and fullerene-like boron solids possesses many novel structural, electronic and thermal properties. The proposed boron nanotubes possess a metallic-like density of states, which are predicted to be relatively stable and have metallic conductivities exceeding those of carbon nanotubes with potential applications in field emission and high-temperature electron devices.[11,12] Single-shell AlB_2 nanotubes were also expected to be

*Project supported in part by the National 863 (Grant No 2007AA03Z305) and 973 (Grant No 2007CB935503) Projects, the National Science Foundation of China (Grant Nos U0734003 and 60571045), and China Postdoctoral Science Foundation.
†Corresponding author. E-mail:hjgao@aphy.iphy.ac.cn

metallic by using density-functional calculations.[13] These new boron and boron-based nanotubes, if synthesized, may have potential applications in nanoelectronics, in field emission device and in nanocomposites where they may impart stiffness, toughness, and strength.

Despite the importance of boron and boron based nanotubes, there were few reports on the experimental synthesis of boron and boron based nanotubes, except a few reports on the synthesis of boron nanowires and nanobelts, and boron based compound nanowires. Amorphous boron nanowires were first fabricated by chemical vapour transport method by using boron, iodine and silicon as precursor, and by radio-frequency magnetron sputtering of the target made of boron and boron oxide, and laser ablating of boron target at high temperature of 1300°C.[4,5,14,15] The β-rhombohedral boron nanowires then were obtained through post-annealing amorphous boron nanowires synthesized by radio-frequency magnetron sputtering.[16] In addition, Otten *et al*[17] straightly synthesized unknown crystalline structure boron nanowires by chemical vapour deposition reaction of diborane (B_2H_6) in Ar gas on the alumina substrates. The α-tetragonal structure boron nanowires have been also fabricated by laser ablation and thermal vapour transport process.[18−21] In the recent years, Wang *et al*[22] and Xu *et al*[23] synthesized another important one-dimensional boron nanomaterial, single crystalline α-tetragonal boron nanobelts by using laser ablation of high-purity boron pellets and by pyrolysis of B_2H_6 at low temperature of 630–750°C. Electrical conductivity of above one-dimensional boron nanomaterials has been measured, and results indicated that the crystalline boron nanowires and boron nanobelts are *p*-type semi-conducting and exhibit electrical properties higher than those of elemental bulk boron.[24,25] Mg doped boron nanobelts then were carried out by vapour diffusion method, and the electrical conductance increased by about a factor of 100 than that of pure boron nanobelts.[26] Boron based compound nanowires have been also fabricated on the base of boron nanowires or straightly synthesized by chemical reaction method. MgB_2 nanowires with the diameter of 50–400 nm were prepared by reacting boron nanowires with Mg vapour in a sealed quartz tube, and the superconductivity of MgB_2 nanowires at 33 K is confirmed by magnetization measurement.[4] Single crystalline LaB_6 nanowires with uniform diameter of about 100 nm and well-defined growth direction were developed by using a chemical vapour deposition method by Qin *et al*.[27] However, as another important one-dimensional boron nanomaterial, few reports about boron nanocones were obtained although it is expected that one-dimensional nanocones should have some better properties than that of nanowires and nanobelts.[28,29] The successful fabrication of boron nanocones will provide a very effective way to fabricate one-dimensional boron based compound nanocones materials by using boron nanocones as the substrate.

In this paper, we prepared the boron nanocones by a simple chemical vapour deposition method, the thermal evaporation of B/B_2O_3 powders precursors in an Ar/H_2 gas mixture at the reaction temperature of 1000–1200°C. The effect of process parameters on boron nanocones growth, such as ratio of $B:B_2O_3$, ratio of H_2:Ar, gas flow rate, catalyst, and synthesis time and temperature has been studied in detail. The corresponding growth mechanism and model of boron nanocones were also postulated. Photoluminescence (PL) of boron nanocones were measured to explore the future possibility applications in optical emitting devices.

2. Experimental

A single-stage furnace is used to synthesize boron nanocones in the experiments.[30] Figure 1 shows a diagram of the apparatus.

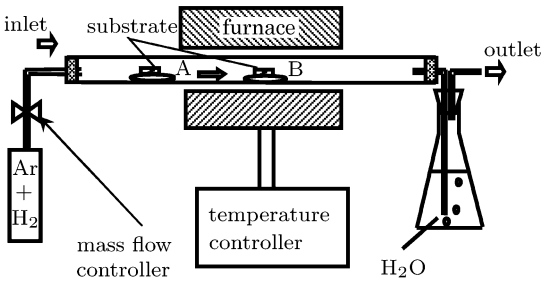

Fig.1. A diagram of apparatus to synthesize the boron nanocones.

2.1. Preparation of Fe_3O_4 and Pd nanoparticles

Fe_3O_4 nanoparticles with diameter less than 10 nm were synthesized by high temperature solution phase reaction.[31] Typically, iron acetylacetonate ($Fe(acac)_3$), 1, 2-dodecandiol, oleic acid and oleylamine were mixed in phenyl ether under the protection of nitrogen. Firstly, the mixture was heated to

200°C. After maintaining the temperature for about 30 minutes, the mixture was heated to about 270°C for 1 h. Then, it was cooled to room temperature naturally, and a large excess of ethanol was added under ambient conditions. After centrifugation and purification, Fe_3O_4 nanoparticles were obtained and dissolved in heptanes. Pd nanoparticles were synthesized by ethylene glycol (EG), H_2PdCl_4, and poly vinyl pyrrolidone (PVP) solution. Firstly, the 10 mL ethylene glycol was placed in a three-neck flask and heated to 150°C for 1 h. Under argon protection, H_2PdCl_4 solution in EG (3 mL, 0.125 M) and PVP solution in EG (3 mL, 1 M) were injected simultaneously into the flask at a rate of 0.5 mL/min. Heating of the reaction mixture was continued for 1 h at 150°C, and cooled to room temperature. The as-prepared solution was precipitated by acetone, and then washed by mixture of ethanol and cyclohexane with volume ratio of 1:5 several times to remove excess PVP and EG. Finally, Pd nanoparticles with diameter less than 10 nm were obtained.

2.2. Fabrication of boron nanocones

Boron powders (99.9%) and boron oxide (B_2O_3) powders (99.99%) in the different weight ratios (pure boron, 4:1, 2:1, 1:1, 1:2, 1:4, and pure B_2O_3) were grounded as precursors, which were charged into the alumina boats, respectively. The Fe_3O_4 or Pd liquid-drops were first spread over Si (111) wafer, a small amount of boron powders then were immerged into the Fe_3O_4 or Pd liquid-drops on Si (111) wafer. A mixture of boron and Fe_3O_4 nanoparticles, or a mixture of boron and Pd nanoparticles coated Si (111) wafer was placed above the alumina boat as the substrate, which remained at out of reaction region (site A) before boron nanocones grew. The temperature, gas flow rate, and evaporation rate of reaction region (site B) could be controlled. The boron nanocones grew by a two-step raising temperature method. In the first procedure, when the temperature of the site B reached 400°C, the sample was transferred from site A to site B rapidly and kept there for 30 min to eliminate the remained oleic acid and oleylamine. Then, the sample was returned from site B to site A. The gas mixtures of Ar and 0, 5%, 10% H_2 flow rate kept up 300 sccm through this procedure. In the second procedure, when the temperature of site B was increased to 1000, 1100, and 1200°C, the sample was transferred from site A to site B rapidly again. The growth of boron nanocones started. The reaction lasted for 1, 30, 60, and 240 min in this procedure under a constant 30, 50, or 100 sccm flow rate of Ar and H_2 gas mixture. During the above two processes, the gas pressure in quartz tube was kept at atmospheric pressure. After the furnace was cooled to room temperature, dark brown or black products were found on the surface of Si(111) substrate.

2.3. Characterization of boron nanocones

Field-emission type scanning electron microscope (SEM) (XL-SFEG, FEI Corp.) was used for morphological observation of boron nanocones. Transmission electron microscopy (TEM) (Tecnai-20, PHILIPS Cop.) and high-resolution transmission electron microscopy (HRTEM) (Tecnai F20, FEI Corp.) with an electron energy loss spectrometer (EELS) were employed to perform the microanalysis of boron nanocones. PL measurements of boron nanocones films were recorded with JY-HR800 spectrometry system with a charge-device (CCD) detector and an optical microscopy system at room temperature. The 532 nm Nb-YAG laser with an output power of 0.9 mW was used for excitation.

3. Results and Discussion

3.1. The effect of process parameters on the products morphology

3.1.1. The effect of ratio of B:B_2O_3

Figure 2 shows SEM images of the products at the different weight ratios of B:B_2O_3 (pure boron, 4:1, 2:1, 1:1, 1:2, 1:4, and pure B_2O_3) with the Fe_3O_4 catalysts at the synthesis temperature of 1100° for 60 min. It can be seen that no boron nanocones were observed for pure boron and weight ratio of 4:1, and some nanometre particles appeared at the surface of sample (Fig.2(a)). Only few boron nanocones were detected on the surface of substrate with the weight ratio decreased to 2:1 (Fig.2(b)). When the weight ratio was decreased to 1:1 and 1:2, high density boron nanocones with several micrometres lengths were observed (Fig.2(c) and 2(d)). Further reducing the weight ratio to 1:4, we can find that the amount of boron nanocones became less (Fig.2(e)), and no boron nanocones were detected for pure B_2O_3 (Fig.2(f)), whose morphology is similar to that of

Fig.2(a). The corresponding relationship of the different process parameters and morphologies of products are listed systemically in Table 1. It denoted that the suitable weight ratio of B:B_2O_3 is very necessary to obtain large scale, high quantity boron nanocones. No boron nanocones growth under only one source material of boron and B_2O_3, indicated that both boron and B_2O_3 may take part in the synthesis reaction of boron nanocones. The effect of boron and B_2O_3 on boron nanocones growth will be discussed in the latter chapter.

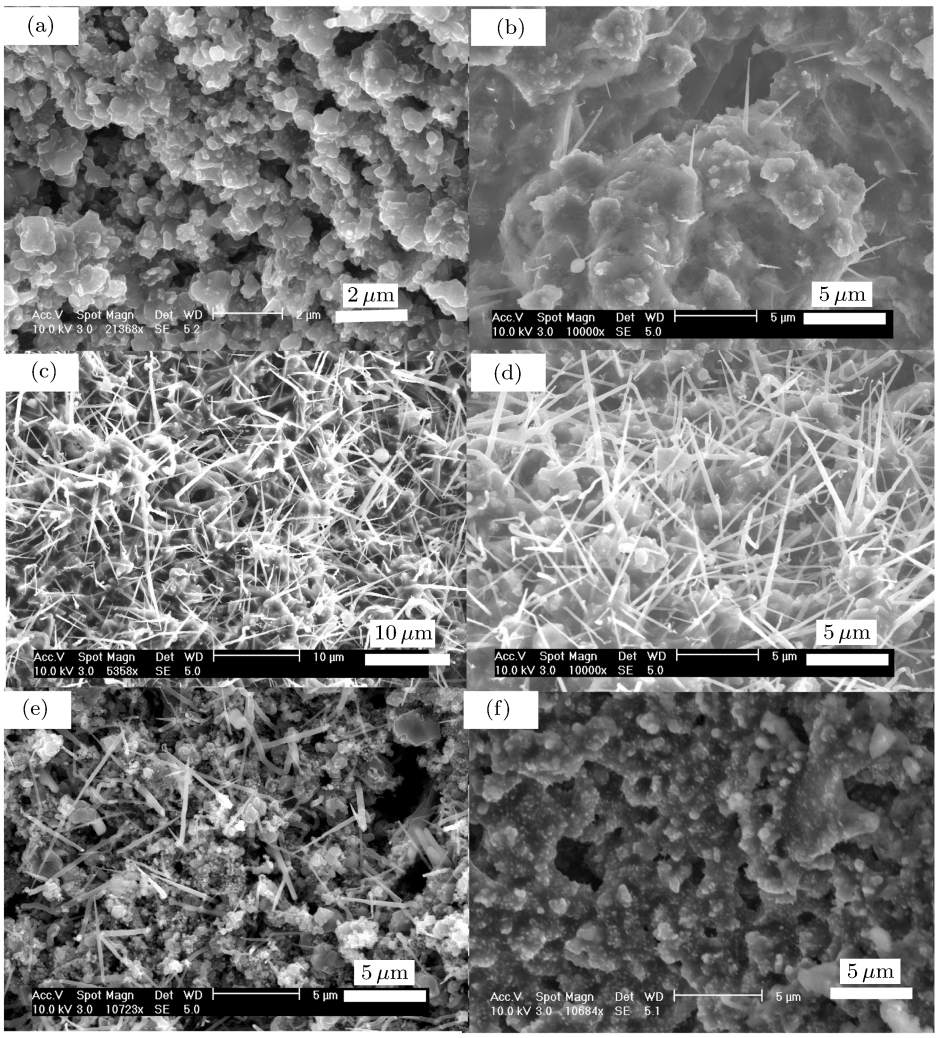

Fig.2. SEM images of the products at the different weight ratios of B:B_2O_3 with the Fe_3O_4 catalysts at the synthesis temperature of 1100°C for 60 min. (a) Pure boron and 4:1. (b) 2:1. (c) 1:1. (d) 1:2. (e) 1:4. (f) Pure B_2O_3.

3.1.2. The effects of ratio of H_2:Ar and gas flow rate

The different volume ratios of H_2:Ar and gas flow rate have been adopted to fabricate boron nanocones. The results show that no boron nanocones were found without the existence of H_2. With increasing the ratio of H_2:Ar to 10%, a large amount of boron nanocones was still detected as same as that for 5% ratio of H_2:Ar. It indicated that H_2 plays a very important role in the formation of boron nanocones. The gas flow rates of 30 and 100 sccm were also used to fabricate boron nanocones. Boron nanocones can form for gas flow rate of 30 sccm. However, boron nanocones were not observed for the gas flow rate of 100 sccm. It is the reason that the reaction source was flowed out for strong gas flow rate of 100 sccm, which led that reaction source from the alumina boat can not reach at the surface of Si(111) substrate with the catalysts, and further not react with the catalysts.

Table 1. The process parameters and corresponding products morphologies.

No	B:B_2O_3 /wt%	H_2:Ar /%	Gas flow rate /sccm	Catalyst	Temperature /°C	Sintering time /min	Morphology
1	Pure B	5	50	Fe_3O_4	1100	60	Some nanometre particles
2	4:1	5	50	Fe_3O_4	1100	60	Some nanometre particles
3	2:1	5	50	Fe_3O_4	1100	60	Several boron nanocones
4	1:1	5	50	Fe_3O_4	1100	60	A large amount of boron nanocones with several micrometres lengths
5	1:2	5	50	Fe_3O_4	1100	60	A large amount of boron nanocones with several micrometres lengths
6	1:4	5	50	Fe_3O_4	1100	60	Few boron nanocones
7	Pure B_2O_3	5	50	Fe_3O_4	1100	60	Similar to exp.1 (no boron nanocones)
8	1:1	0	50	Fe_3O_4	1100	60	Similar to exp.1 (no boron nanocones)
9	1:1	10	50	Fe_3O_4	1100	60	Similar to exp.4 (A large amount of boron nanocones with several micrometres lengths)
10	1:1	5	30	Fe_3O_4	1100	60	Similar to exp.4 (A large amount of boron nanocones with several micrometres lengths)
11	1:1	5	100	Fe_3O_4	1100	60	Similar to exp.1 (no boron nanocones)
12	1:1	5	50	Pd	1100	60	Few boron nanowires with several micrometres lengths
13	1:1	5	50	Fe_3O_4	900	60	Few boron nanocones
14	1:1	5	50	Fe_3O_4	1000	60	Similar to exp.4 (A large amount of boron nanocones)
15	1:1	5	50	Fe_3O_4	1200	60	Similar to exp.4 (A large amount of boron nanocones)
16	1:1	5	50	Fe_3O_4	1100	1	Many boron nanocones for initial growth stage
17	1:1	5	50	Fe_3O_4	1100	30	A large amount of boron nanocones for completely growth stage
18	1:1	5	50	Fe_3O_4	1100	240	A large amount of boron nanocones for completely growth stage with some tip curves.

3.1.3. The effect of catalysts

Figures 3(a) and 3(b) show the SEM images of products using the Pd nanoparticles catalysts. Few boron nanowires were observed with a larger catalyst droplet on the top of nanowire than that of related nanowire. The lengths of nanowires are several micrometres, and the diameters of the nanowires are about 100 nm. Boron nanocones can not be obtained through adjusting the process parameters, showing that the growth of boron nanocones needs the special catalysts.

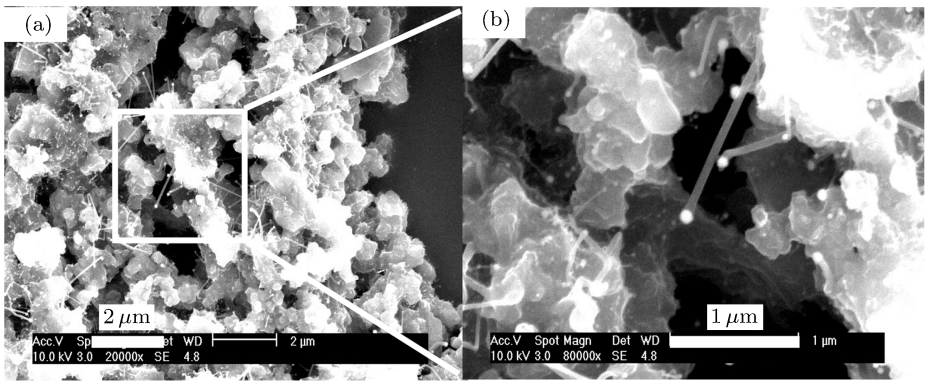

Fig.3. SEM images of products using Pd nanoparticles catalysts.

3.1.4. The effects of synthesis time and temperature

Figure 4 shows the typical SEM images of boron nanocones at the different synthesis time of 1, 30, and 240 minutes, respectively. The cone-shaped rods were observed, as shown in Figs.4(a) and 4(b). The top diameters of boron rods are about several hundreds nanometres, and the aspect ratio is less than 10. At every one top of these rods, there is a droplet whose

diameter is slightly smaller than that of related rod. It denoted that the period is the initial stage for boron nanocones growth, and boron nanocones do not grow up completely. With the time increased to above 30 min, it can be found that the boron nanocones have completely growth up (Fig.4(c)), even some tip curves appeared at the tops of boron nanocones for the synthesis time of 240 min (Fig.4(d)). The different synthesis temperatures of 900, 1000, 1100, and 1200°C have been also changed to fabricate the boron nanocones, and results indicated that boron nanocones only can form above 1000°C.

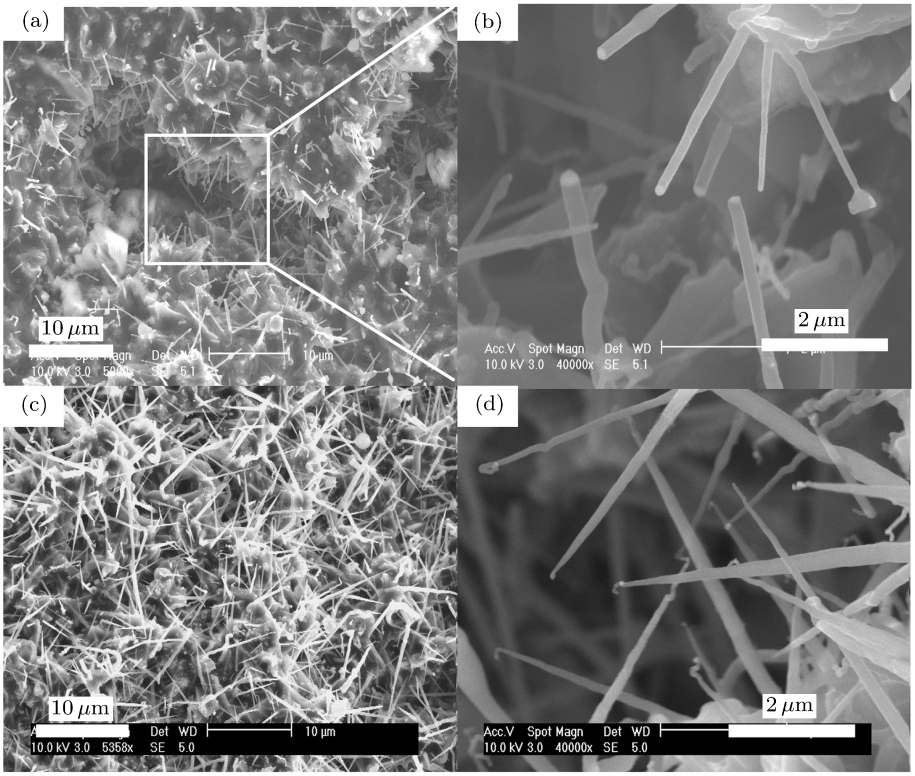

Fig.4. SEM images of products at the different synthesis time. (a) and (b) 1 min. (c) 30 min. (d) 240 min.

3.2. Composition, structure, and growth mechanism of boron nanocones

3.2.1. Composition and structure of boron nanocones

Figures 5(a) and 5(b) show the SEM images of one boron nanocone for initial and completely growth stages, respectively. The length of boron nanocone for initial growth stage is about 3 μm. The root and top diameters of boron nanocone are about 400 nm and 200 nm, respectively (Fig.5(a)). There is a hemisphere catalyst droplet on the top of boron nanocone whose diameter is a little smaller than that of related cone. The top diameter of boron nanocone become sharp for completely growth stage boron nanocone (Fig.5(b)). Further sample characterization was carried out by using TEM and HRTEM. Figure 5(c) is TEM image of boron nanocone for initial growth stage. Figure 5(d) and 5(e) show HRTEM images of middle and top of the nanocone. It can be clearly seen that demarcation line exists at the top of boron nanocone, showing that the boron nanocone is growing up. Figure 5(f) shows TEM image of boron nanocone for completely growth stage. Electron diffraction was done on the different parts of nanocone to determine its structure. The electron diffraction pattern for the different parts of nanocone is same, as shown in the inset of Fig.5(f). The calculated lattice constants are a=0.876 nm and c=0.508 nm, which coincide closely with the values of α-tetragonal boron from the JCPDS database (73-0511).[32] This structure is in agreement with that of boron nanobelts by pyrolysis of B_2H_6 at low temperature of 630–750°C.[23] Figures 5(g) and 5(h) show the HRTEM images of middle and top of

nanocone. The sharp tip was detected at the top, and the preferential growth direction was determined to be the [001] direction. Chemical compositions of the different parts of nanocone were analysed by EELS in another publication.[33] Only characteristic peak of boron was observed, no oxygen, iron or other impurities were detected from the middle of boron nanocone. However, a very small amount of iron was detected by EELS spectrum from the front part of nanocone. This indicated that some iron, as the catalyst, located at the front part of boron nanocone.

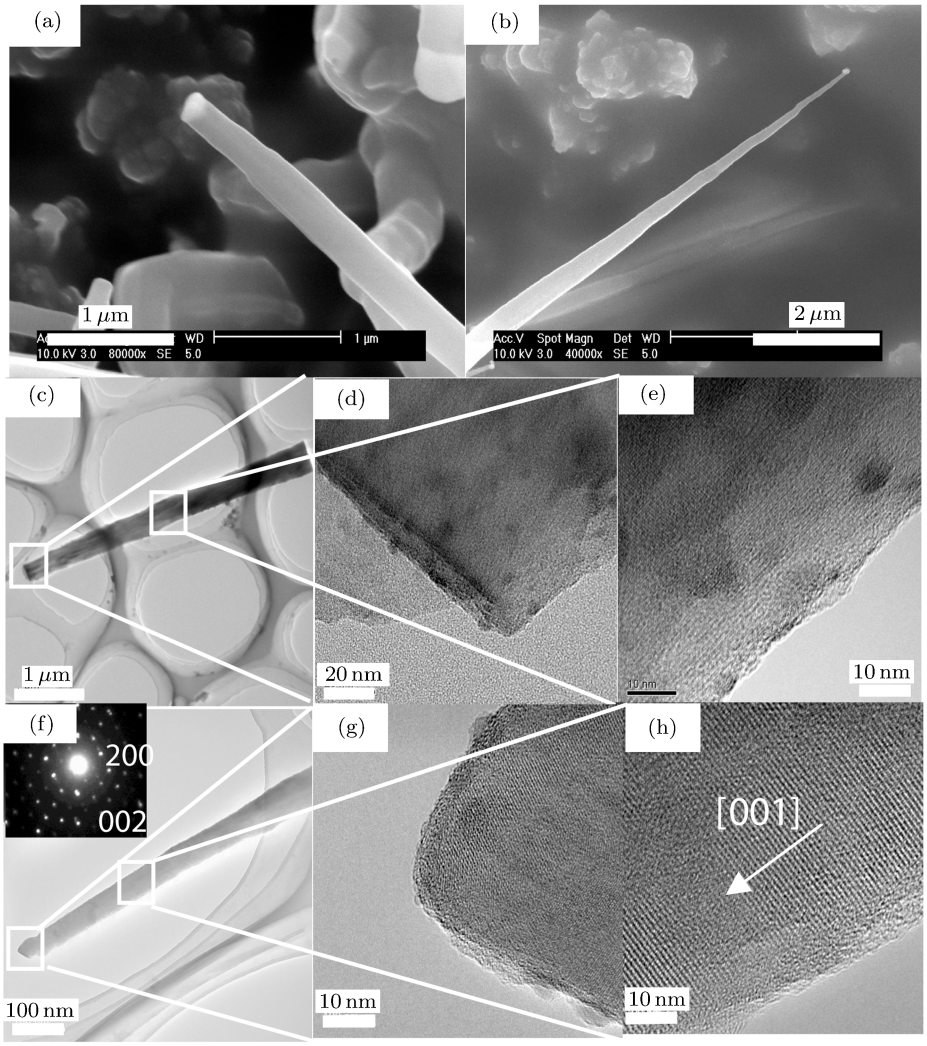

Fig.5. (a) and (b) SEM images for boron nanocone for initial and completely growth stages. (c) TEM image of boron nanocone for initial growth stage. (d) and (e) HRTEM images of middle and top of boron nanocone for initial growth stage. (f) TEM image of boron nanocone for completely growth stage, the inset is the corresponding electron diffraction pattern. (g) and (h) HRTEM images of middle and top of boron nanocone for completely growth stage.

3.2.2. Growth mechanism of boron nanocones

First of all, it should be noted that H_2 is a key element to prepare boron nanocones because the boron nanocones only can be obtained under H_2 existence. In addition, boron nanocones can not be formed by using only one source material of boron and B_2O_3, suggesting that the H_2 should have a reduction reaction with some substoichiometric boron oxides (BO_x) produced from boron and B_2O_3, not with pure B_2O_3. Thirdly, in our experiments, Fe_3O_4 nanoparticles were employed as the catalysts to fabricate the boron nanocones. We also tried to synthesize boron nanocones without the Fe_3O_4 catalysts, but

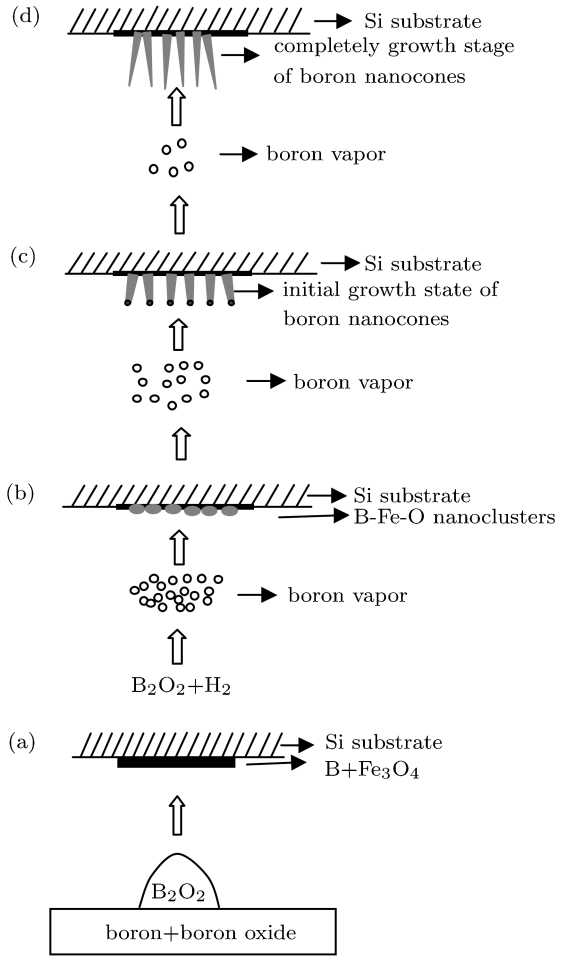

Fig.6. A schematic model of the boron nanocones growth.

one-dimensional boron nanomaterials were observed on the surface of Si(111) substrates. Moreover, the fact that iron was detected in the EELS spectrum only at the tops of the boron nanocones suggests that a vapour–liquid–solid (VLS) mechanism is the most probable growth mechanism. The similar VLS mechanism was also adopted to explain the growth of the crystalline boron nanowires, when Ni and Co nanoparticles served as the catalysts.[18] Figure 6 shows a schematic model of the boron nanocones growth. Firstly, B_2O_3 with low melting point of 450°C in the alumina boat transforms from solid to liquid as the temperature increases from 400 up to above 1000°C. During the above process, B_2O_3 liquid which reacts with solid boron in the alumina boat forms dimeric boron monoxide (B_2O_2) vapour (Fig.6(a)),[34]

$$2B_2O_3 + 2B \rightarrow 3B_2O_2. \quad (1)$$

Meanwhile, iron, boron and oxygen on the surface of Si(111) substrate serve as the energetically favoured sites for the condensation and precipitation of the reactant vapour. Iron, boron and oxygen nanoclusters are formed on the surface of Si(111) substrate. The B_2O_2 vapour reacts with H_2 on the surface of the Si (111) substrate to form the boron vapour (Fig.6(b)),

$$B_2O_2 + 2H_2 \rightarrow 2B + 2H_2O. \quad (2)$$

The condensation and precipitation of the boron species from the hot vapour take place on these iron, boron and oxygen nanoclusters. One-dimensional boron nanomaterials growth begins after boron species become supersaturated in the iron, boron and oxygen nanoclusters. At the initial stage, the abundant reactants provide sufficient boron vapour pressure to promote a rapid growth of boron to form big nanodroplets in a short period of time. As the reaction goes on, pressure of the boron vapour is reduced gradually due to the limited supply from the sources, leading to a transition from the nanodroplets into the nanocones (Fig.6(c)). The oxygen outdiffuses to the outer layer, and escapes into vacuum. Finally, boron nanocones are formed on the Si(111) substrate (Fig.6(d)).

3.3. Photoluminescence properties of boron nanocones

Figure 7 shows the room-temperature PL spectrum of boron nanocones film under 532 nm light excitation. One broad PL emission peak was clearly observed at the central wavelength of about 650 nm. According to energy level diagram of boron, we can found that PL emission peak at the centre of about 800 nm should be obtained corresponding to energy level difference of valence band and conductor band for pure boron.[35] The 650 nm PL emission peak has shift compared with the PL of bulk boron, which may be the effect of quantum confinement in the synthesized boron nanocones.[36] The similar phenomenon has been found in many nanomaterials.[37] For example, PL emission peak of SiC nanowires has blue-shift compared with that of bulk SiC.[38] Broad PL spectra are often due to strong electron photon interactions or distributions of energy levels of luminescence centres. The origin of the broadness is considered to be the distributions of the energy levels, which result from the rather complicated crystalline structure of boron. The visible emission properties of boron nanocones are of significant interest for their potential visible optical

emitting device applications.

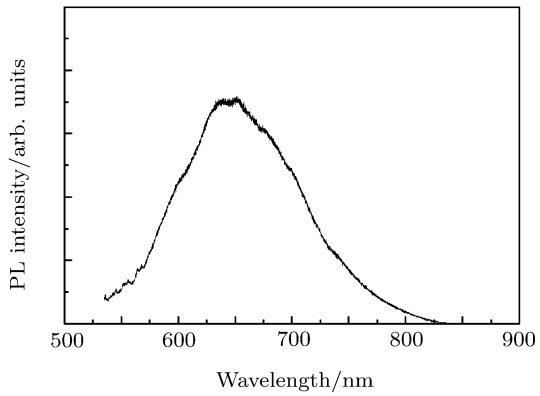

Fig.7. The room temperature PL spectrum of boron nanocones film under 532 nm light excitation.

4. Conclusions

Large scale, high density single crystalline α-tetragonal boron nanocones have been fabricated by a simple chemical vapour deposition method. The lengths of boron nanocones are several micrometres, and the diameters of these nanocone tops are in a range of 50–100 nm. The VLS mechanism is the main formation mechanism of boron nanocones. Boron nanocones have one broad PL emission at the central wavelength of about 650 nm when 532 nm light excitation is applied at room temperature. The good PL characteristics are attributed to the special properties of boron nanocones, which are promising candidates for applications in optical emitting devices.

References

[1] Appell D 2002 *Nature* **419** 553
[2] Xia Y, Yang P, Sun Y, Wu Y, Mayers B, Gates B, Yin Y, Kim F and Yan H 2003 *Adv. Mater.* **15** 353
[3] Xiao C W, Yang H T, Shen C M, Li Z A, Zhang H R, Liu F, Yang T Z, Chen S T and Gao H J 2005 *Chin. Phys.* **14** 2269
[4] Wu Y Y, Messer B and Yang P D 2001 *Adv. Mater.* **13** 1487
[5] Cao L M, Zhang Z, Sun L L, He M, Wang Y Q, Li Y C, Zhang X Y, Li G, Zhang J and Wang W K 2001 *Adv. Mater.* **13** 1701
[6] Matkovich V I 1977 *Boron and Refractory Borides* (New York: Springer)
[7] Emin D 1987 *Phys. Today* **40** 55
[8] Kohn J A 1960 *Boron Synthesis, Structure, and Properties* (New York: Plenum Press) p3
[9] Eremets M, Struzhkin V, Mao H K and Hemley R 2001 *Science* **293** 272
[10] Larbalestier D, Cooley L and Rikel1 M 2001 *Nature* **410** 186
[11] Boustani I and Quandt A 1997 *Europhys. Lett.* **39** 527
[12] Boustani I, Quandt A, Hernandez E and Rubio A 1999 *Chem. Phys.* **110** 3176
[13] Quandt A, Liu A Y and Boustani I 2001 *Phys. Rev.* B **64** 125422
[14] Cao L M, Hahn K, Wang Y Q, Scheu C, Zhang Z, Gao C X, Li Y C, Zhang X Y, Sun L L and Wang W K 2002 *Adv. Mater.* **14** 1294
[15] Meng X M, Hu J Q, Jiang Y, Lee C S and Lee S T 2003 *Chem. Phys. Lett.* **370** 825
[16] Wang Y Q and Duan X F 2003 *Appl. Phys. Lett.* **82** 272
[17] Otten C J, Loune O R, Yu M F, Cowley J M, Dyer M J, Ruoff R S and Buhro W E 2002 *J. Am. Chem. Soc.* **124** 4564
[18] Zhang Y J, Ago H, Yumura M, Komatsu T, Ohshima S, Uchida K and Iijima S 2002 *Chem. Commun.* **23** 2806
[19] Zhang Y J, Ago H, Yumura M, Ohshima S, Uchida K, Komatsu T and Iijima S 2004 *Chem. Phys. Lett.* **385** 177
[20] Yun S H, Dibos A, Wu J Z and Kim D K 2004 *Appl. Phys. Lett.* **84** 2892
[21] Yun S H, Wu J Z, Dias A, Gao X and Karlsson U O 2005 *Appl. Phys. Lett.* **87** 113109
[22] Wang Z K, Shimizu Y, Sasaki T, Kawaguchi K, Kimura K and Koshizaki N 2003 *Chem. Phys. Lett.* **368** 663
[23] Xu T T, Zheng J G, Wu N Q, Nicholls A W, Roth J R, Dikin D A and Ruoff R S 2004 *Nano lett.* **4** 963
[24] Wang D W, Lu J G, Otten C J and Buhro W E 2003 *Appl. Phys. Lett.* **83** 5280
[25] Kirihara K, Wang Z, Kawaguchi K, Shimizu Y, Sasaki T, Koshizaki N, Soga K and Kimura K 2005 *Appl. Phys. Lett.* **86** 212101
[26] Kirihara K, Wang Z, Kawaguchi K, Shimizu Y, Sasaki T, Koshizaki N, Hyodo H, Soga K and Kimura K 2005 *J. Vac. Sci. Technol.* B **23** 2510
[27] Zhang H, Zhang Q, Tang J and Qin L C 2005 *J. Am. Chem. Soc.* **127** 2862
[28] Xu C X and Sun X W 2003 *Appl. Phys. Lett.* **83** 3806
[29] Zhang Z X, Yuan H J, Zhou J J, Liu D F, Luo S D, Gao Y, Wang J X and Xie S S 2006 *J. Phys. Chem.* B **110** 8566
[30] Cao P J, Gu Y S, Liu F, Liu H W, Zhang Q F, Wang Y G and Gao H J 2004 *Acta Phys. Sin.* **53** 854 (in Chinese)
[31] Yang T Z, Shen C S, Li Z A, Zhang H R, Xiao C W, Chen S T, Xu Z C, Shi D X, Li J Q and Gao H J 2005 *J. Phys. Chem.* B **109** 23233
[32] JCPDS-International Centre for Diffraction Data, PCPDFWIN 2003 V.2.4
[33] Wang X J, Tian J F, Yang T Z, Bao L H, Hui C, Liu F, Shen C M, Gu C Z, Xu N S and Gao H J 2007 *Adv. Mater.* **19** 4480
[34] Ma R Z and Bando Y 2002 *Chem. Phys. Lett.* **364** 314
[35] Hori A, Tada T and Kimura K 1998 *J. Phys. Soc. Jpn.* **67** 4279
[36] Choi H J, Johnson J J, He R, Lee S K, Kim F, Pauzaauski P, Goldgerger J, Saykally R J and Yang P 2003 *J. Phys. Chem.* B **107** 8721
[37] Chen S, Chen D Y, Chen K J, Feng D, Han P G, Huang X F, Li W, Ma Z Y, Qian B, Xia Z Y and Xu J 2007 *Chin. Phys.* **16** 1410
[38] Wang X J, Tian J F, Bao L H, Hui C, Yang T Z, Liu F, Xu N S, Shen C M and Gao H J 2007 *J. Appl. Phys.* **102** 014309